Supporting Information

Construction of Circularly Polarized Luminescence Sensor Based on Self-Assembly of Carbon Dots and G-quartet Chiral Nanofibers

Dong Wang, Zhiwei Zhang, Xuetao Yan, Tianliang Li, Yingying Chen, Zhenzhen Li and Lingyan Feng**

E-mail: zhenzhen_li@shu.edu.cn; lingyanfeng@t.shu.edu.cn

Characterization Techniques

XPS analysis were carried out at room temperature on a Kratos Axis Ultra DLD instrument manufactured by KRATOS corporation (Manchester, UK). All XPS spectroscopy were tested at least three times and were repeatable. FTIR analysis were carried out at room temperature on a Nicolet iS50 FT-IR spectrometer manufactured by Thermo Fisher Scientific Corporation (Massachusetts, USA). Samples were prepared by KBr tableting method and the spectrum was collected with 1 cm^{-1} resolution and 512 numbers of scan conditions in the range of 400-2000 nm. All FT-IR spectra were tested at least three times and were repeatable. XRD analysis were carried out at room temperature on a D2 PHASE X-ray diffraction system manufactured by Bruker AXS corporation (Karlsruhe, Germany). Samples were all freeze-dried before XRD analysis and the XRD patterns were measured in 2θ range from 20 to 70 degrees with a step size of $\Delta\theta = 0.1$ degree(Cu–Kα radiation, 40 kV, 40 mA, $\lambda = 1.5418$ Å). All XRD patterns were measured at least three times and were repeatable. SEM images were conducted at room temperature on a GEMINI 300 field emission scanning electron microscope with SE2 detector manufactured by Zeiss corporation (Oberkochen, Germany). All samples were evenly spread on the conductive adhesive to form a thin layer and left to dry before scanning. All SEM images were measured at least three times and were repeatable. TEM images were conducted at room temperature on a Tecnai G2 F20 S-Twin TMP electron microscope manufactured by FEI corporation (Oregon, USA) with an accelerating voltage of 200 kV. The N-S-CDs solution is dripped on the copper mesh

to dry naturally before testing. All TEM images were measured at least three times and were repeatable. Fluorescence spectra were obtained at room temperature on a FS5 spectrofluorometer manufactured by Edinburgh instruments corporation (Edinburgh, UK) using a quartz cuvette with 1.0 cm path length. Both excitation and emission scanning slits are 1 nm and dwell time is 0.3s. And the step size of both excitation and emission spectra were 1 nm. All fluorescence spectra were measured at least three times and were repeatable.

UV-Vis absorption spectra were obtained at room temperature on a Lambda 750 spectrophotometer manufactured by Perkin-Elmer corporation (Massachusetts, USA) using a quartz cuvette with 1.0 cm path length. Spectra were scanned from 200-800 nm with a step size of 1 nm at a scan speed of 100 nm/min, and the bandwidths for incident light beam is 2 nm. All UV-Vis absorption spectra were tested at least three times and were repeatable. CD spectra were measured at room temperature on a J-1500 Circular Dichroism Spectrometer attached with a temperature controller manufactured by JASCO corporation (Tokyo, Japan) using a quartz cuvette with 1.0 mm path length. Samples were sandwiched between two 1mm quartz plates. Spectra were scanned from 200-800 nm with a data pitch of 0.2 nm at a scan speed of 200 nm/min, and the bandwidth for incident light beam is 5 nm and D.I.T. is 2 sec. All CD spectra were measured at least three times and were repeatable. CPL spectra were measured at room temperature on a CPL-300 spectrometer attached with a temperature controller manufactured by JASCO corporation (Tokyo, Japan) using a quartz cuvette with 1.0 mm path length. Samples were sandwiched between two 1mm quartz plates. The measure range of CPL spectrum is 390-600 nm with a data pitch of 0.2 nm and an excitation wavelength at 350 nm at a scan speed of 100 nm/min, and the bandwidths for incident and emission light beam are both 16 nm and D.I.T. is 4 sec. Each CPL spectrum was an average of three measurements and were repeatable. Optical and fluorescent microscopy images were taken at room temperature on a FV3000 microscope manufactured by Olympus corporation (Tokyo, Japan). Samples are uniformly dispersed on glass slides for imaging observation. Fluorescence imaging was performed at an excitation wavelength of 405 nm.

Calculation of the absolute photoluminescence quantum yield (QY)

The QY of N-S-CDs was measured in absolute terms by direct excitation in a calibrated integrating sphere of the Edinburgh FS-5 Fluorescence Spectrometer with a quantum efficiency measurement system. And the absolute photoluminescence QY can be calculated by using the following equation:

$$QY = \frac{\int I_{emission}}{\int I_{blank} - \int I_{sample}}$$

$I_{emission}$ was the photoluminescence emission spectrum of sample, collected using the integrating sphere; I_{sample} was the spectrum of the light used to excite sample, collected using the integrating sphere; I_{blank} was the spectrum of the light used for excitation with only the solvent in the sphere, collected using the sphere. The solvent in this experiment was ultrapure water.

Fluorescence lifetime assay

The lifetime of N-S-CDs was measured by an Edinburgh Optoelectronic Time-Resolved Fluorometer based on the Time-Resolved Single Photon Detection System (TCSPC). The samples were all excited by a diode laser with an emission wavelength of 365 nm. The decay curve was accumulated to 2000 times until the highest peak. The decay data were fitted by an exponential model (residual error $\chi^2 \leq 1.3$):

$$R(t) = \sum_i B_i e^{-\frac{t}{\tau_i}}$$

where *R(t)* is the fluorescence intensity at time t, *Bi* is the *i*-th pre-exponential factor at time t, and τ_i is the *i*-th fluorescence lifetime. The mean fluorescence lifetime (τ_{av}) is calculated by the following formula:

$$\tau_{av} = \frac{\sum \alpha_i \tau_i^2}{\sum \alpha_i \tau_i}$$

where α_i represents the proportion of life τ_i.

Supplementary figures

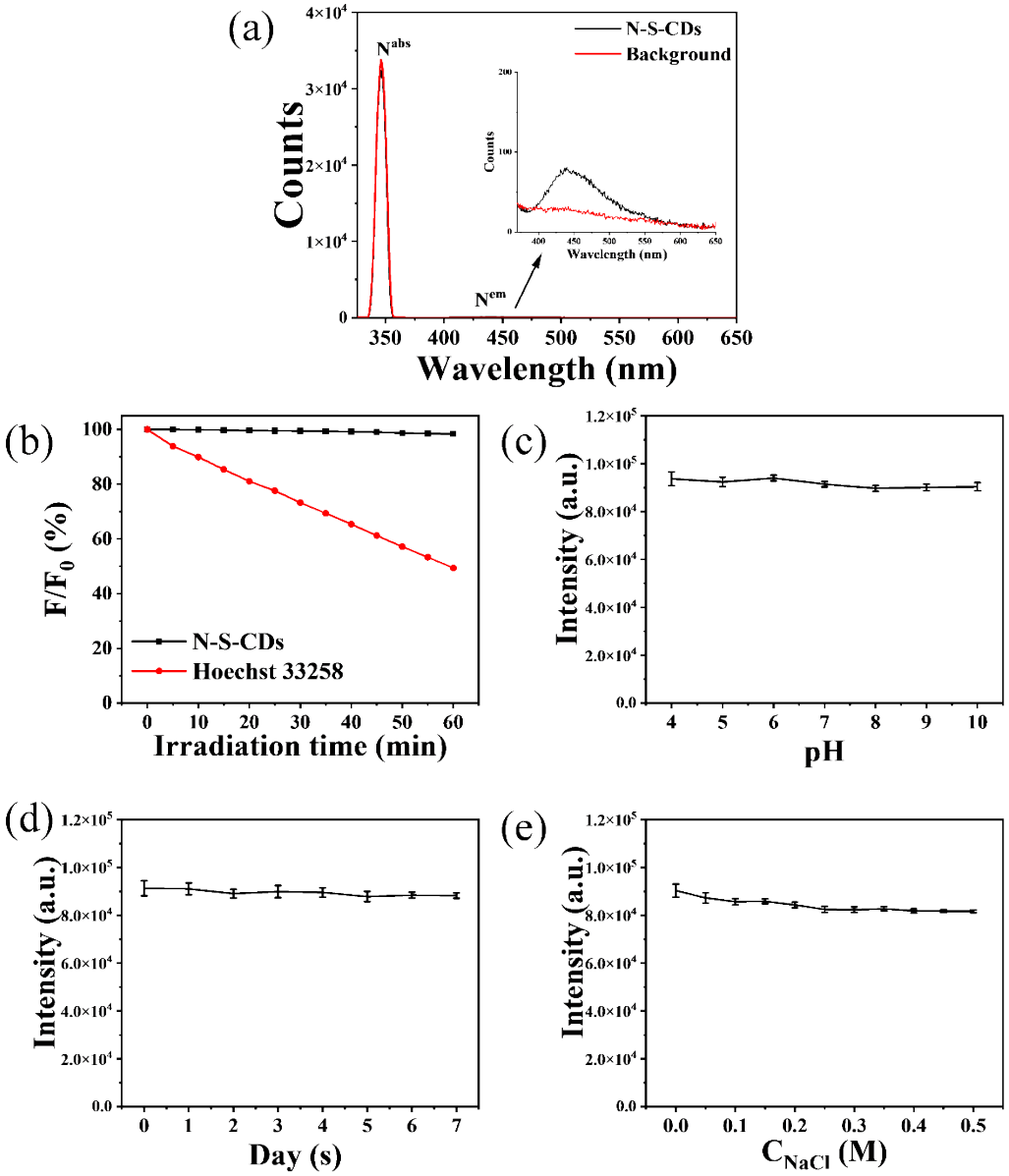

Fig. S1. (a) The Quantum Yield (QY) of N-S-CDs; (b) The effect of irradiation time on the PL intensity of N-S-CDs and commercial dye Hoechst 33258 ($C_{Hoechst\ 33258}$=10 μM); The effect of (c) pH value, (d) Standing time; (e) salt concentrations on the PL strength of N-S-CDs.

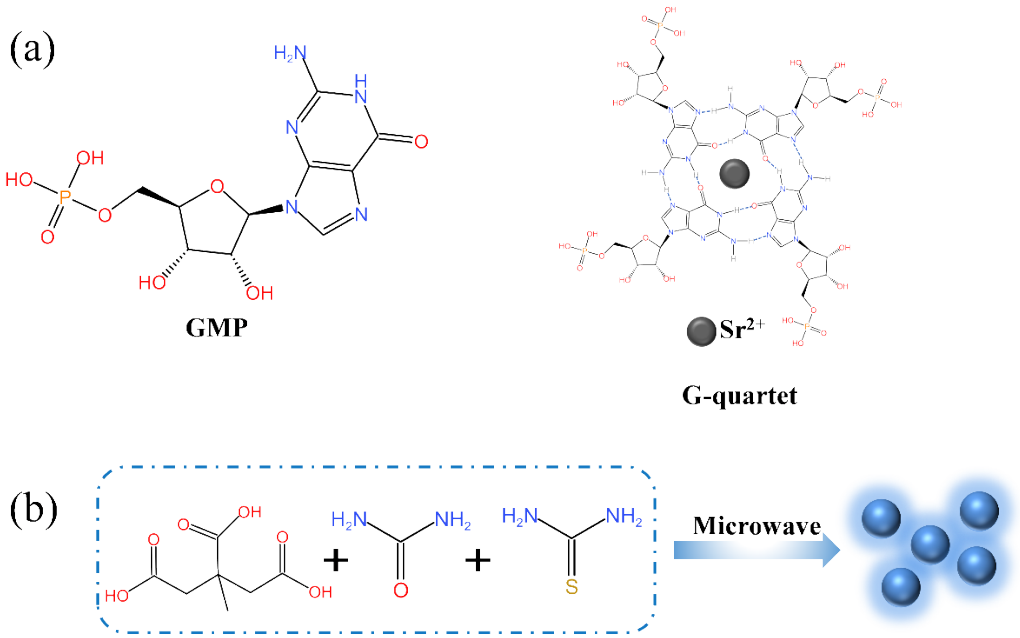

Fig. S2. (a) The structure of GMP and G-quartet; (b) The synthesis of N-S-CDs.

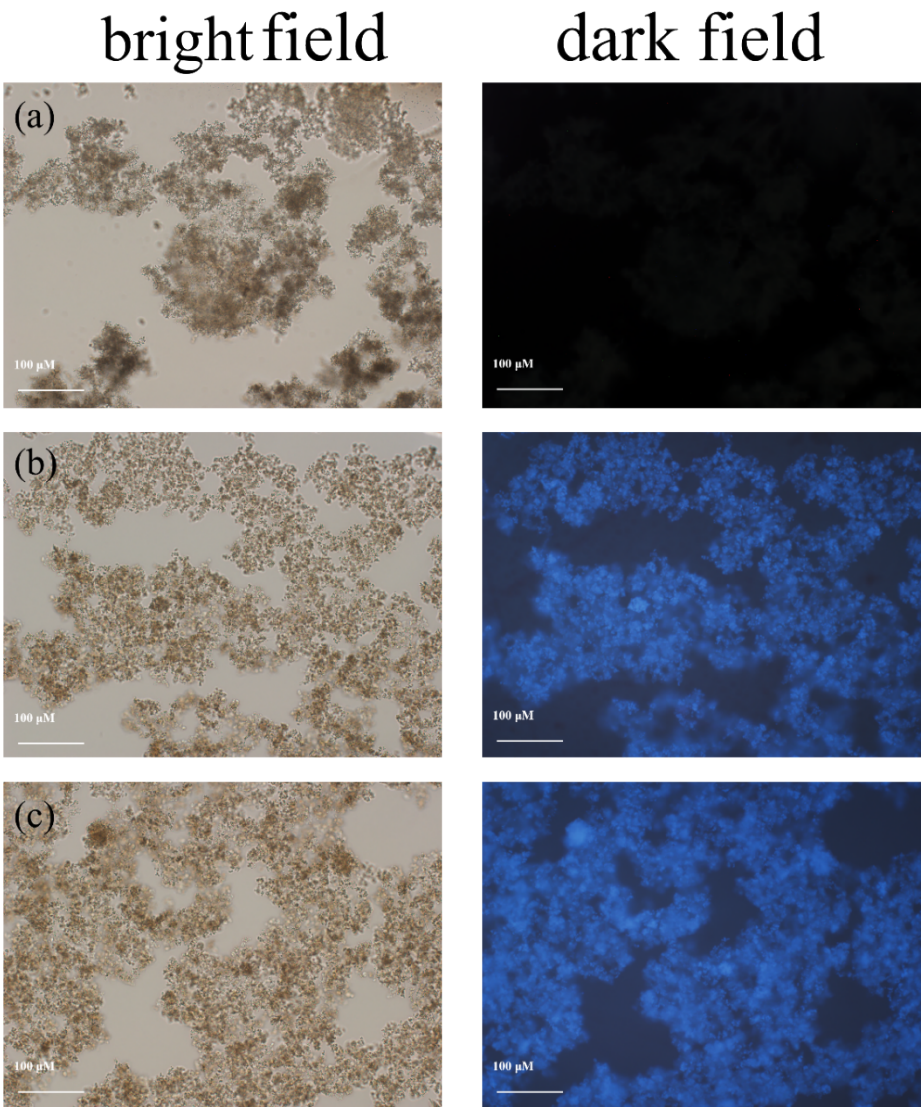

Fig. S3. Fluorescence confocal microscopy images of (a) R-fiber; (b) right-handed N-S-CDs/g-fiber; (c) left-handed N-S-CDs/g-fiber (left: bright field, right: dark field).

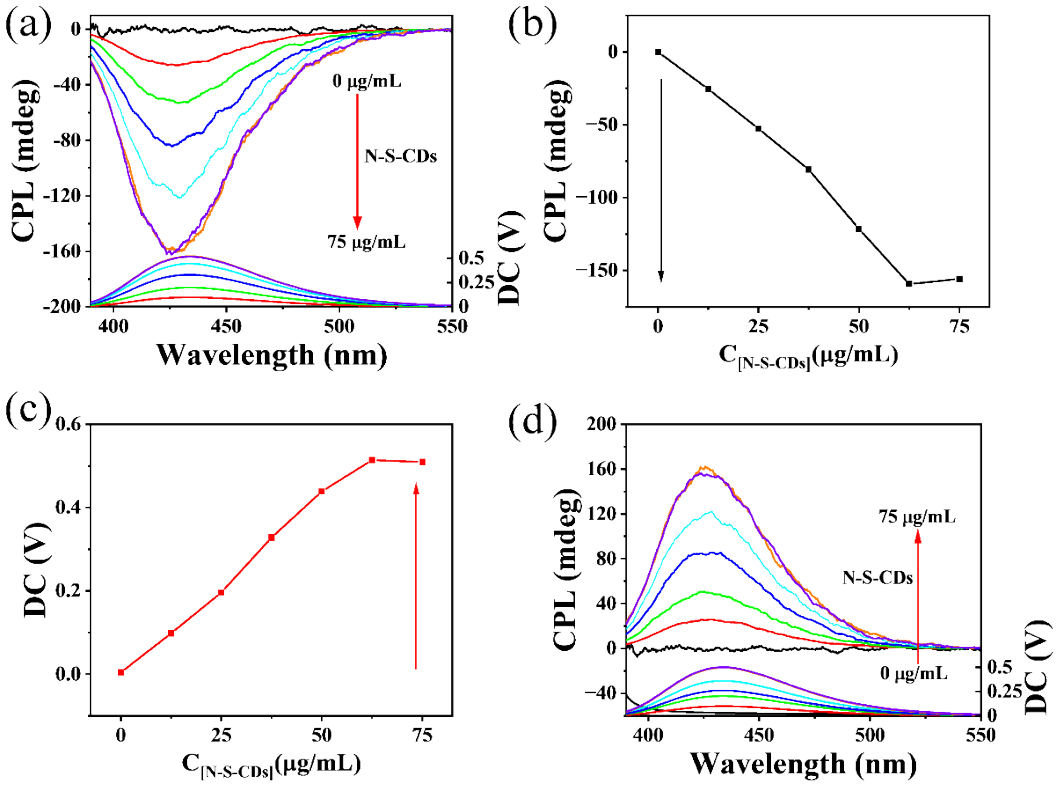

Fig. S4. (a) CPL spectra of the right-handed N-S-CDs/g-fiber at different concentrations of N-S-CDs (0, 12.5, 25, 37.5, 50, 62.5, 75 μg/mL); (b) The CPL strength and (c) DC value of the right-handed N-S-CDs/g-fiber as a function of the concentration of assembled N-S-CDs; (d) CPL spectra of the left-handed N-S-CDs/g-fiber at different concentrations of N-S-CDs (0, 12.5, 25, 37.5, 50, 62.5, 75 μg /mL).

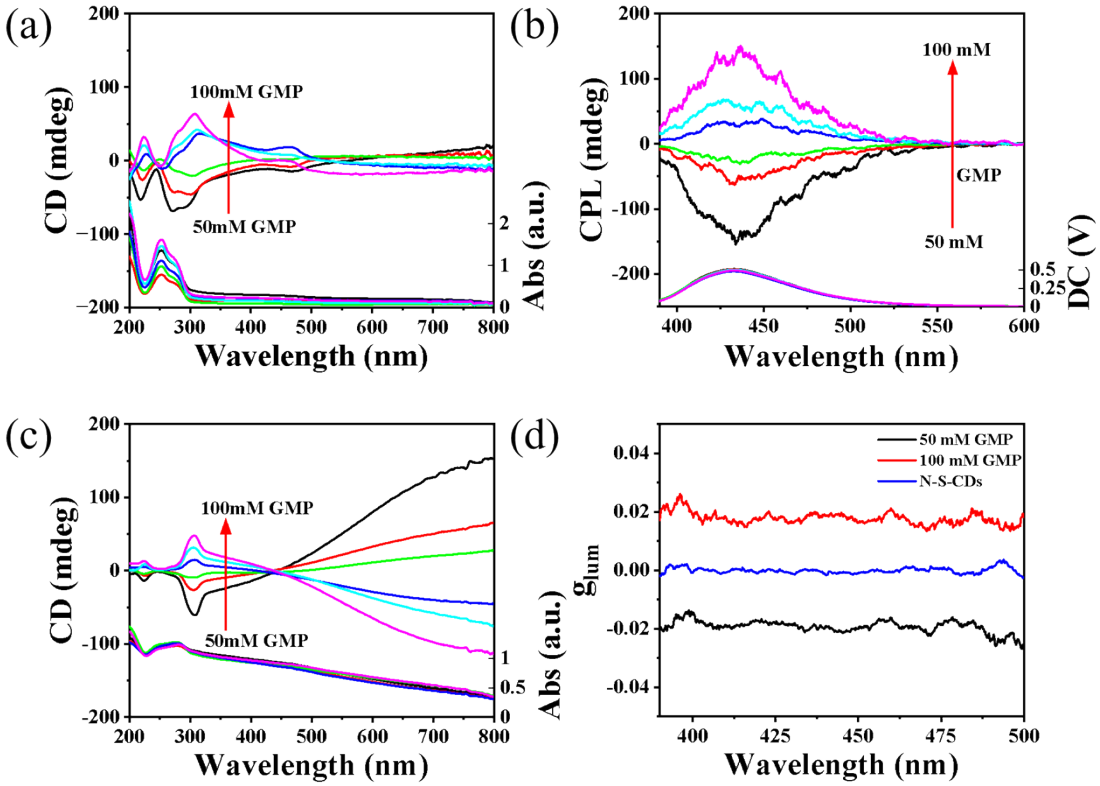

Fig. S5. (a) CD spectra of g-fiber at varying GMP concentrations (50, 60, 70, 80, 90, 100 mM) and corresponding Sr^{2+} concentrations (8, 9.6, 11.2, 12.8, 14.4, 16 mM); (b) CPL spectra; (c) CD spectra of N-S-CDs/g-fiber at varying GMP concentrations (50, 60, 70, 80, 90, 100 mM) and corresponding Sr^{2+} concentrations (8, 9.6, 11.2, 12.8, 14.4, 16 mM); (d) g_{lum} value curve chart.

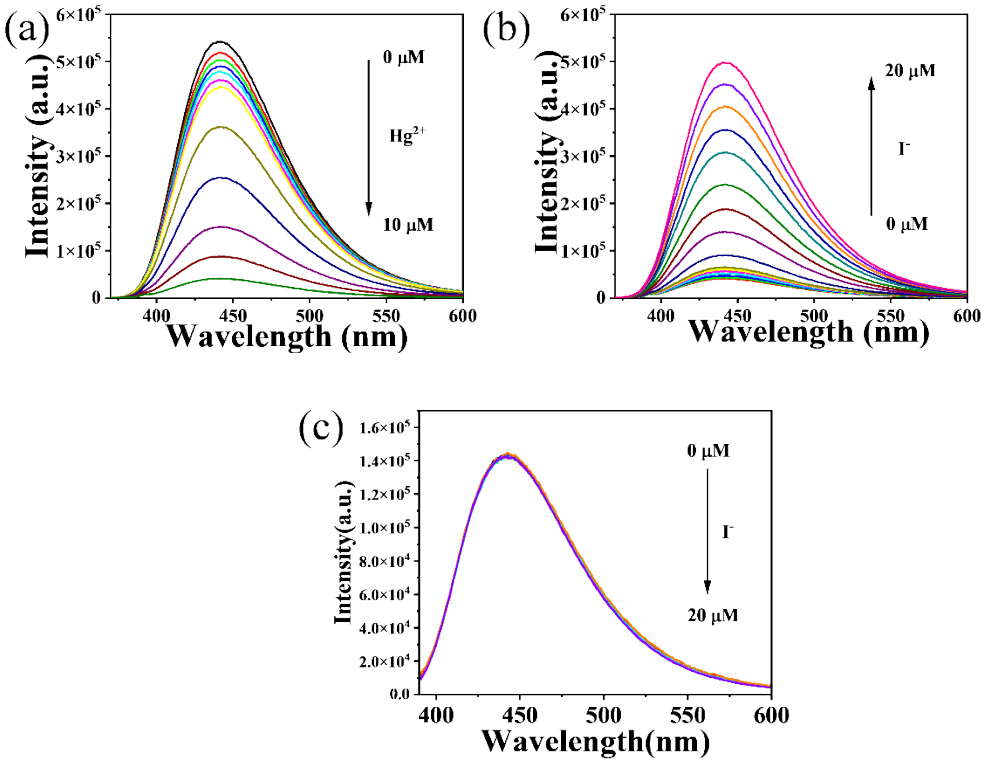

Fig. S6. (a) PL spectra of N-S-CDs at different concentrations of Hg^{2+}(0, 0.1, 0.2, 0.4, 0.6, 0.8, 1, 2, 4, 6, 8, 10 μM); (b) PL spectra of N-S-CDs-Hg^{2+} system at different concentrations of I^- (.0, 0.1, 0.2, 0.4, 0.6, 0.8, 1, 2, 4, 6, 8, 10, 12, 14, 16, 18, 20 μM); (c) PL spectra of N-S-CDs at different concentrations of I^- (0, 0.1, 0.2, 1, 5, 10, 15, 20 μM) while in the absence of Hg^{2+}.

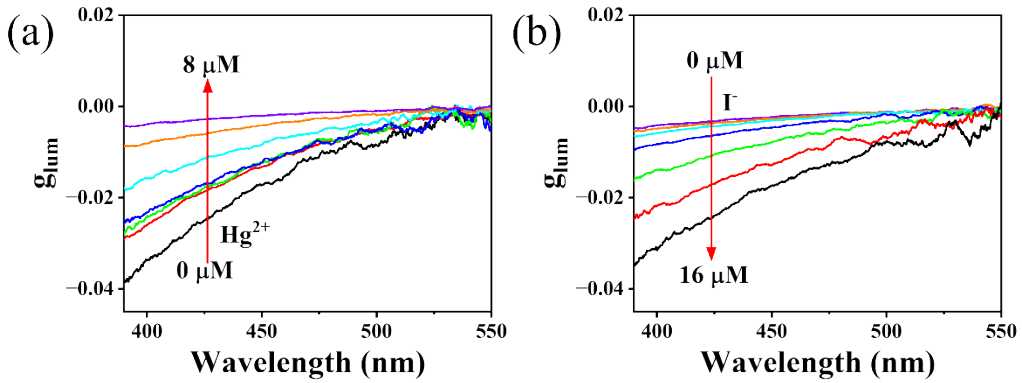

Fig. S7. (a) g_{lum} value curve chart of the right-handed N-S-CDs/g-fiber with increasing concentrations of Hg^{2+} (0, 0.1, 0.5, 1, 3, 8 μM); (b) g_{lum} value curve chart of the right-handed Hg^{2+}-N-S-CDs/g-fiber with increasing concentrations of I^- (0, 0.2, 1, 2, 6, 10, 16 μM).

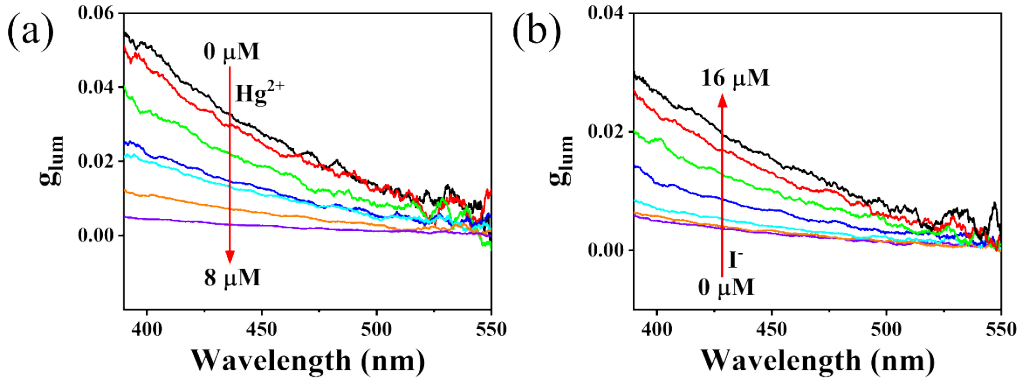

Fig. S8. (a) g_{lum} value curve chart of the left-handed N-S-CDs/g-fiber with increasing concentrations of Hg^{2+} (0, 0.1, 0.5, 1, 3, 8 μM); (b) g_{lum} value curve chart of the left-handed Hg^{2+}-N-S-CDs/g-fiber with increasing concentrations of I^- (0, 0.2, 1, 2, 6, 10, 16 μM).

Table S1. Comparison of Different Analysis Methods and Materials for Detecting Hg^{2+} Performance.

Method	Materials	Hg^{2+} detection		Ref.
		LOD (μM)	Detection range (μM)	
Fluorometric	N-doped CDs	0.41	0−50	1[1]
	Graphene quantum dots	0.1	0.8−9	2[2]
	N,S/C-dots	2	0−40	3[3]
Colorimetric	carbon nanodots	0.38	2−20	4[4]
	berberine-based compounds	5.4	0−500	5[5]
	SN-CDs/AuNPs	0.5	0.5−15	6[6]
Electrochemical	Hemin	0.005	1−5	7[7]
	BC-Au	0.489	0.5−6	8[8]
Electrochemiluminescence	$Ru(bpy)_3^{2+}$/TSC	0.03	0.5−60	9[9]
CPL	N-S-CDs/g-fiber	0.0835	0.1−8	This work

Table S2. Comparison of Different Analysis Methods and Materials for Detecting I^- Performance.

Method	Materials	I^- detection		Ref.
		LOD (μM)	Detection range (μM)	
Fluorometric	DNA-Au/Ag-NCs	0.3	0−10	10[10]
	SC-dots	0.18	1−100	11[11]
	Au NCs	0.4	1−10	12[12]
	CdSe quantum dots	0.28	0.28−40	13[13]
HPLC-DAD	phosphatidylcholine column	0.179	3.9−78.8	14[14]
Capillary Electrophoresis	α-cyclodextrin	0.06	0.2−4	15[15]
Electrochemical	modified platinum electrode	3.9	20−70	16[16]
Flow-injection chemiluminescence	carbon nanodots	0.35	3−100	17[17]
CPL	N-S-CDs/g-fiber	0.1428	0.2−16	This work

References

1. L. Cai, Z. Fu and F. Cui, *Journal of Fluorescence*, 2020, **30**, 11-20.
2. B. Wang, S. Zhuo, L. Chen and Y. Zhang, *Spectrochimica Acta Part A: Molecular and Biomolecular Spectroscopy*, 2014, **131**, 384-387.
3. L. Li, B. Yu and T. You, *Biosensors and Bioelectronics*, 2015, **74**, 263-269.
4. L. Wang, L. Yu, H. Ge, Y. Bu, M. Sun, D. Huang and S. Wang, *Microchemical Journal*, 2022, **175**, 107181.
5. S. Ruan, Y. Zhang, S. Wu, Y. Gao, L. Yang, M. Li, Y. Yang, Z. Wang and S. Wang, *Inorganic Chemistry Communications*, 2021, **132**, 108847.
6. C. Lu, H. Ding, Y. Wang, C. Xiong and X. Wang, *Nanotechnology*, 2021, **32**, 155501.
7. Y. Lai, Y. Ma, L. Sun, J. Jia, J. Weng, N. Hu, W. Yang and Q. Zhang, *Electrochim. Acta*, 2011, **56**, 3153-3158.
8. H. Pu, S. Ruan, M. Yin, Q. Sun, Y. Zhang, P. Gao, X. Liang, W. Yin and H.-b. Fa, *Microchemical Journal*, 2022, **181**, 107711.
9. T. H. Barkae, F. Yuan, T. H. Fereja, S. A. Kitte, X. Ma, W. Zhang and G. Xu, *Electrochim. Acta*, 2021, **380**, 138171.
10. Z. Li, R. Liu, G. Xing, T. Wang and S. Liu, *Biosensors and Bioelectronics*, 2017, **96**, 44-48.
11. J. Chen, X. Liu, X. Hou, Y. Chen, F. Xing and L. Feng, *Analytical and Bioanalytical Chemistry*, 2020, **412**, 2893-2901.
12. M. Wang, Z. Wu, J. Yang, G. Wang, H. Wang and W. Cai, *Nanoscale*, 2012, **4**, 4087-4090.
13. Z. B. Shang, Y. Wang and W. J. Jin, *Talanta*, 2009, **78**, 364-369.
14. M. Tatarczak-Michalewska, J. Flieger, J. Kawka, W. Flieger and E. Blicharska, *Journal*, 2019, **24**.
15. A. N. d. Macedo, K. Teo, A. Mente, M. J. McQueen, J. Zeidler, P. Poirier, S. A. Lear, A. Wielgosz and P. Britz-McKibbin, *Analytical Chemistry*, 2014, **86**, 10010-10015.
16. T. R. I. Cataldi, A. Rubino and R. Ciriello, *Analytical and Bioanalytical Chemistry*, 2005, **382**, 134-141.
17. S. Han, B. Liu, Z. Fan, L. Zhang and F. Jiang, *Luminescence : the journal of biological and chemical luminescence*, 2017, **32**, 1192-1196.